A nitric oxide/cysteine interaction mediates the activation of soluble guanylate cyclase

Nathaniel B. Fernhoff[a,1], Emily R. Derbyshire[a,1,2], and Michael A. Marletta[a,b,c,3]

Departments of [a]Molecular and Cell Biology and [b]Chemistry, University of California, Berkeley, CA 94720; and [c]California Institute for Quantitative Biosciences and Division of Physical Biosciences, Lawrence Berkeley National Laboratory, Berkeley, CA 94720

Contributed by Michael A. Marletta, October 1, 2009 (sent for review August 22, 2009)

Nitric oxide (NO) regulates a number of essential physiological processes by activating soluble guanylate cyclase (sGC) to produce the second messenger cGMP. The mechanism of NO sensing was previously thought to result exclusively from NO binding to the sGC heme; however, recent studies indicate that heme-bound NO only partially activates sGC and additional NO is involved in the mechanism of maximal NO activation. Furthermore, thiol oxidation of sGC cysteines results in the loss of enzyme activity. Herein the role of cysteines in NO-stimulated sGC activity investigated. We find that the thiol modifying reagent methyl methanethiosulfonate specifically inhibits NO activation of sGC by blocking a non-heme site, which defines a role for sGC cysteine(s) in mediating NO binding. The nature of the NO/cysteine interaction was probed by examining the effects of redox active reagents on NO-stimulated activity. These results show that NO binding to, and dissociation from, the critical cysteine(s) does not involve a change in the thiol redox state. Evidence is provided for non-heme NO in the physiological activation of sGC in context of a primary cell culture of human umbilical vein endothelial cells. These findings have relevance to diseases involving the NO/cGMP signaling pathway.

thiol | TC-1 | cGMP | S-nitrosation | redox

Cardiovascular disease is the leading cause of death in the United States and the enzyme soluble guanylate cyclase (sGC) is a therapeutic target for treatment of the disease. sGC is the central protein in the nitric oxide (NO)/cGMP signaling cascade, a pathway that mediates diverse physiological functions including vasodilation, platelet aggregation, and neurotransmission (1–3). Although >20 years have passed since sGC was identified as the primary eukaryotic NO receptor (4), our understanding of the molecular details of sGC activation by NO continues to evolve.

sGC is a heterodimeric hemoprotein consisting of an 80-kDa α subunit and a 70-kDa β subunit. In mammals, there are two isoforms for each subunit, and the N-terminal domain ($\approx$200 residues) of the β subunit binds a heme cofactor. The unliganded enzyme exhibits a low level of cGMP production and is referred to as the basal state. NO coordination to the sGC heme has been thoroughly investigated and was presumed to cause the conversion of the unactivated basal enzyme to the activated NO-bound enzyme. Indeed, coordination of NO to the sGC heme cofactor correlates with a large increase of sGC activity (5, 6); however, we and others have recently demonstrated that NO ligation to the heme is not sufficient to fully activate sGC (7, 8).

NO initially binds to the sGC heme with picomolar affinity (9, 10), inducing a moderate activation of the enzyme (7, 8). This low activity form of the enzyme maintains a 1:1 stoichiometry of NO to sGC, and we refer to it henceforth as the 1-NO state. This 1-NO state exhibits a slow rate of NO dissociation (11, 12) and, as a consequence, this form of the enzyme can be stably isolated away from free NO in solution (7, 8, 13). The subsequent addition of excess NO to the 1-NO state further stimulates sGC to a high activity form that we refer to as the xsNO state. The xsNO state is spectrally identical to the 1-NO state, but it only persists in the presence of excess NO. When NO is removed from solution, the high activity of the xsNO state rapidly reverts to the low activity of the 1-NO state. Thus, all three sGC states (basal, 1-NO, and xsNO) can be prepared and studied in vitro (7, 8). Importantly, these results define two different states of purified sGC with heme bound NO (7, 8), one with a high activity and one with a low activity.

Further evidence for a non-heme NO binding site was obtained by blocking the heme site with the tight-binding ligand butyl isocyanide, and then showing that NO still activated the enzyme (14). The dependence of sGC function on the non-heme NO binding site draws specific attention to its nature. There is precedent for reversible gaseous ligand binding in proteins involving a non-heme metal (15) or a hydrophobic binding pocket (16); however, sGC is isolated with only the heme iron, and other hydrophobic diatomic gasses such as N_2, CO, and O_2 fail to stimulate the enzyme. A plausible mechanism that could account for the selectivity of NO is through a transient reaction with a cysteine thiol.

In this work, we investigate the function of cysteines in the mechanism of non-heme NO activation and demonstrate a physiological role for non-heme NO activation. Our results suggest that oxidative damage can block the non-heme NO binding site, consequently inhibiting NO stimulation of sGC in vivo. Importantly, these results provide a mechanistic explanation for observations of sGC inhibition by thiol modifying reagents and oxidants (17–19), and it is therefore relevant toward addressing the molecular mechanism of NO tolerance (19, 20), a disease state characterized by a decreased sensitivity to NO in cardiovascular tissue. Additionally, each sGC state (basal, 1-NO, and xsNO) may be a unique target for therapeutic intervention in diseases involving sGC dysfunction.

Results and Discussion

Kinetic Characterization of sGC States. It is known that the 1-NO state exhibits a low level of activity compared with the xsNO state (7, 8); however, a kinetic characterization of these different states has not been reported. Therefore, to further investigate the mechanism of non-heme NO activation of sGC, the V_{max} and K_m for GTP turnover was determined for the basal, 1-NO, and xsNO sGC states (Table 1). In the 1-NO state, NO coordination only to the heme leads to an increase in the V_{max} and a reduction in the K_m when compared with the basal state. Non-heme NO binding to the 1-NO state further increases V_{max} with no change in the K_m. This increase in V_{max} from the 1-NO state to the xsNO state indicates a shift to a more catalytically competent form of the enzyme upon NO binding to the non-heme site. Because the 1-NO state is activated above the basal state, NO may be classified as a

Author contributions: N.B.F., E.R.D., and M.A.M. designed research; N.B.F. and E.R.D. performed research; N.B.F., E.R.D., and M.A.M. analyzed data; and N.B.F., E.R.D., and M.A.M. wrote the paper.

The authors declare no conflict of interest.

Freely available online through the PNAS open access option.

[1]N.B.F. and E.R.D. contributed equally to this work.

[2]Present address: Department of Biological Chemistry and Molecular Pharmacology, Harvard Medical School, Boston, MA 02446.

[3]To whom correspondence should be addressed at: QB3 Institute, University of California, 570 Stanley Hall, Berkeley, CA 94720-3220. E-mail: marletta@berkeley.edu.

This article contains supporting information online at www.pnas.org/cgi/content/full/0911083106/DCSupplemental.

Table 1. Kinetic parameters of NO-stimulated sGC states

sGC state	V_{max}, nmol·min^{-1}·mg^{-1}	K_m, μM
Basal	14.7 ± 1.3	360 ± 130
xsNO	3610 ± 90	46 ± 6
1-NO	64.1 ± 3.2	46 ± 13

Rates acquired at 25 °C.

non-essential activator for the binding to both the heme and non-heme sites. Therefore, each NO binding event induces a distinct conformational change in the active site.

Non-Heme NO Activation Is Mediated by Cysteine(s). To examine the involvement of sGC cysteines in the mechanism of NO activation, the effect of a thiol reactive reagent on enzyme activity was tested. In these experiments rat $\alpha1\beta1$ sGC was recombinantly expressed in a Sf9/baculovirus system and purified to homogeneity. Purified protein was then treated with the thiol reactive probe methyl methanethiosulfonate (MMTS), which modifies thiols through the formation of methyl disulfides (Eq. **1**).

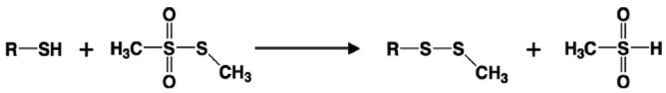

[1]

Because this reaction yields a disulfide product, it is reversible with thiol reductants like DTT. We found that MMTS inhibited NO stimulated sGC activity (Fig. 1*A*), but electronic absorption spectroscopy showed that MMTS did not prevent the formation of the ferrous-nitrosyl complex (Fig. S1). This MMTS-treated ferrous-nitrosyl complex was not stimulated by treatment with additional NO, but the allosteric activator YC-1 was able to activate the protein. YC-1 is an indazole derivative that weakly activates the basal enzyme, but strongly stimulates sGC activity when a ligand is coordinated to the heme (14, 21, 22). The observation of a MMTS-treated ferrous-nitrosyl complex demonstrates that thiol modification does not interfere with NO binding to the heme. Additionally, MMTS (≥100 μM) did not inhibit basal sGC activity (Fig. 1*B*), which shows that the protein did not denature with MMTS treatment and that essential catalytic residues were not modified. MMTS inhibition of sGC was fully reversible by DTT (Fig. 1*C*), demonstrating that the protein structure is not irreversibly damaged by the reaction. These results show that MMTS specifically inhibits the activation of sGC that results from NO binding.

Interestingly, NO stimulation of MMTS-treated sGC resulted in activity that is similar to that of the low-activity 1-NO form of the enzyme (Fig. 1*D*). The observation that MMTS specifically inhibits NO stimulation led us to investigate whether cysteine modification by MMTS inhibits non-heme NO binding. To address this question, MMTS was titrated against sGC and NO stimulated activity was measured (Fig. 1*E*). NO stimulated activity is inhibited at low μM MMTS and is zero order in MMTS between 15 and 100 μM. At concentrations >100 μM, an irreversible loss in both basal and NO stimulated activity was observed. Therefore, high concentrations of MMTS lead to a general, nonspecific inhibition of sGC (17). However, the observation of a saturated range of MMTS inhibition implicates a discrete set of cysteines in the mechanism of non-heme NO activation. This saturating effect of MMTS leaves the enzyme synthesizing cGMP at a rate that matches that of the 1-NO species. If modification caused a nonspecific disruption of catalysis, the protein would be completely inhibited at saturating concentrations of MMTS. Also, because MMTS-treated sGC was stimulated by the combination of both NO and YC-1

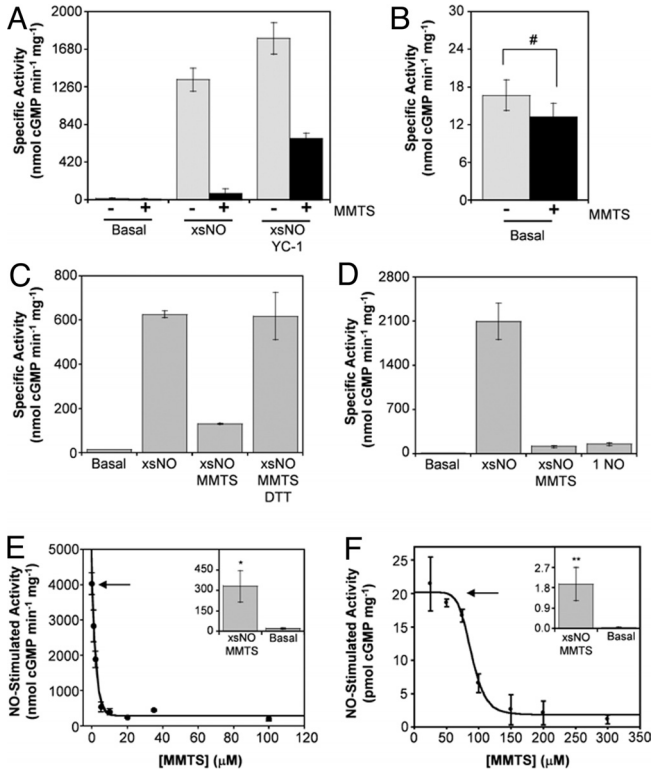

Fig. 1. MMTS inhibition of NO-stimulation sGC activity in vitro and in vivo. (*A*) MMTS inhibits cGMP synthesis of NO-stimulated sGC (xsNO), but YC-1 activates the MMTS-treated protein in the presence of excess NO. (*B*) MMTS does not inhibit basal sGC activity to a statistically significant extent. (*C*) MMTS inhibition of sGC is reversible by DTT. (*D*) MMTS-treated sGC is stimulated by NO to a level comparable to the activity of the 1-NO state. (*E*) Titration of MMTS against NO-stimulated sGC activity shows MMTS inhibition saturates at a level that is statistically greater than basal sGC activity (*Inset*). (*F*) Titration of MMTS against NO-stimulated sGC activity shows inhibition in PC12 cells and this inhibition saturates at a level that is statistically greater than the GC activity in the absence of NO (*Inset*). The arrow indicates maximal sGC activity in the presence of excess NO (*E* and *F*). Data are presented as means ± SD. #, $P = 0.27$; *, $P < 0.00015$; **, $P < 0.025$ compared with basal activity with purified protein (*E*) or PC12 cells (*F*), assessed by an unpaired *t* test.

(Fig. 1*A*), MMTS does not sterically hinder the transition to the high activity state. Therefore, our observation that MMTS-treated sGC maintains partial NO stimulation, combined with the observation that MMTS-treated sGC binds NO at the heme, suggests that the transition from the 1-NO state to the xsNO state is impaired by cysteine modification. Thus, MMTS blocks the cysteine(s) that constitute the non-heme NO binding site.

To assess the role of cysteines in regulating NO activation in vivo, MMTS inhibition of sGC activity in PC12 cells, a rat tumor cell line that endogenously expresses sGC (23) was examined (Fig. 1*F*). Similar to purified protein, the NO stimulated sGC activity exhibited a zero order dependence on MMTS between 100 and 300 μM. This indicates that reduced cysteines are necessary for activation beyond the 1-NO level of stimulation in vivo. The range of zero order activity in PC12 cells differs from purified protein, likely owing to endogenous intracellular reductants. Additionally, because thiol modification with MMTS inhibits NO stimulated activity in vivo, it is possible that other reactants (more specifically intracellular oxidants) may inhibit cGMP production by reaction with the same cysteine. In fact, we have observed sGC inhibition in vitro with molecular oxygen as well as the thiol alkylating reagent *N*-ethyl maleimide (NEM) (Fig. S2). Because both reactive oxygen species and decreased sGC activity are associated with cardiovascular disease (24), it is an attractive hypothesis that cysteine oxidation of the non-heme NO binding site causes symptoms in some forms of the

BIOCHEMISTRY

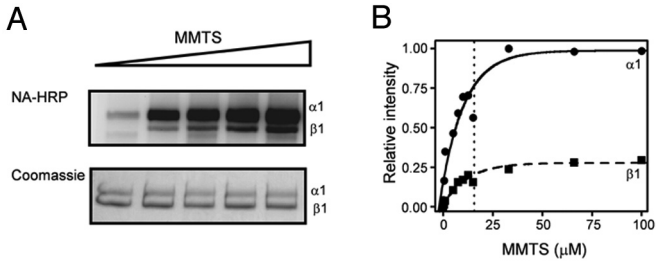

Fig. 2. MMTS labeling of sGC subunits. (*A*) MMTS labeling of sGC cysteines was visualized by Western blot analysis. Cysteines on both α1 and β1 react with MMTS. (*B*) Densitometry of labeled bands reveals a linear relationship between labeling and the concentration of MMTS until labeling saturates [α1 EC_{95} = 34 ± 7 μM (circles); β1 EC_{95} = 36 ± 5 μM (squares)]. The dotted vertical line indicates the saturation of MMTS inhibition of NO-stimulated activity (IC_{95} = 16 ± 2 μM).

disease. This cysteine oxidation would not affect cGMP production in either the basal or 1-NO sGC states but would significantly impair that derived from the xsNO state. These results provide a causative molecular mechanism to observations that cysteine oxidation correlates with reduced sGC activity (17–19).

Characterization of sGC Cysteines Labeled by MMTS. Because the reaction of MMTS with sGC restricts activation beyond the 1-NO state, we sought to estimate the stoichiometry of this reaction. By labeling sGC cysteines with MMTS and then exchanging the methyl disulfide modification for a biotin tag, the extent of the MMTS reaction can be readily visualized (Fig. 2*A*) and quantified (Fig. 2*B*). The MMTS reaction with sGC saturates (α1 EC_{95} = 34 ± 7 μM; β1 EC_{95} = 36 ± 5 μM) and the labeling intensity can be used to estimate the number of MMTS-reactive cysteines by standardizing the labeling intensity to that of denatured sGC reacted with excess MMTS, where all cysteine residues are expected to react (20 cysteines in α1 and 14 in β1) (Fig. S3). This analysis projects that 16 ± 3 cysteines on α1 and 10 ± 1 cysteines on β1 react with MMTS under native conditions. Furthermore, at the minimally sufficient MMTS concentration to fully inhibit sGC (IC_{95} = 16 ± 2 μM, dotted vertical line Fig. 2*B*), MMTS has reacted with 12 ± 2 cysteines on α1 and 8 ± 1 cysteines on β1. Saturation of NO stimulated activity occurs at a lower concentration than the saturation of labeling, suggesting that the cysteine(s) of the non-heme NO binding site is more reactive to MMTS. To map the cysteines that are reactive to MMTS, the MMTS-treated sGC was proteolyzed with trypsin. Analysis of the digests by mass spectrometry identified several MMTS-reactive residues (Table 2). The key residue(s) comprising the non-heme NO binding site is likely contained within the set of MMTS-modified cysteines.

Table 2. sGC cysteines modified by MMTS

Subunit	Residue	Observed peptide
α 1	175	QSSHC*QEAER[†]
α 1	609	FESC*SVPR[†‡]
α 1	628	DC*PGFVFTPR[†‡]
β 1	174	SEEC*DHTQFLIEEK[†‡]
β 1	214	ISPYTFC*K[†‡]
β 1	292	LEC*EDELTGAEISC*LR[‡]
β 1	303	LEC*EDELTGAEISC*LR[‡]

The concentration of MMTS was 20 μM and the numbering corresponds to rat α1β1. C* indicates MMTS-modified cysteine.
[†]Identified by MALDI-TOF/TOF.
[‡]Identified by two-dimensional LC MS/MS.

The NO/Cysteine Interaction Is Reversible in the Absence and Presence of Redox Active Reagents. In the cellular milieu, there is an abundance of both oxidants and reductants, and, as a consequence, instances of cysteine oxidation are frequently reversed by endogenous reductants. Likewise, commonly used assay buffers for in vitro experiments also contain oxidants in the form of O_2 and reductants in the form of DTT. To test the redox chemistry of the NO/cysteine interaction in sGC, the effect of these redox active reagents on NO-mediated cysteine oxidation and enzyme activation was examined.

Nitrosothiols are gaining recognition as biologically relevant post-translational modifications (25). We sought to determine whether S-nitrosation could be responsible for NO induced sGC activation. As mentioned above, S-nitrosation is an oxidative addition of NO to a thiol that requires a redox partner to act as an electron sink, and most often oxygen serves this role in vitro (Eq. **2**):

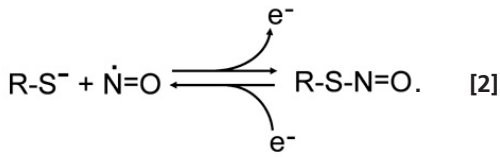

[2]

Indeed, the aerobic addition of NO to sGC produces nitrosothiols (Fig. 3*A*) (19) while concurrently stimulating the enzyme several hundred fold (Fig. 3*B*). If the activating species were a nitrosothiol, then conditions that prevent S-nitrosation must also prevent NO stimulation. However, under anaerobic conditions and in the absence of reductant, NO-stimulated sGC was neither S-nitrosated nor inhibited (Fig. 3 *A* and *B*). Furthermore, because NO activated sGC to the same extent with and without O_2, the mechanism of

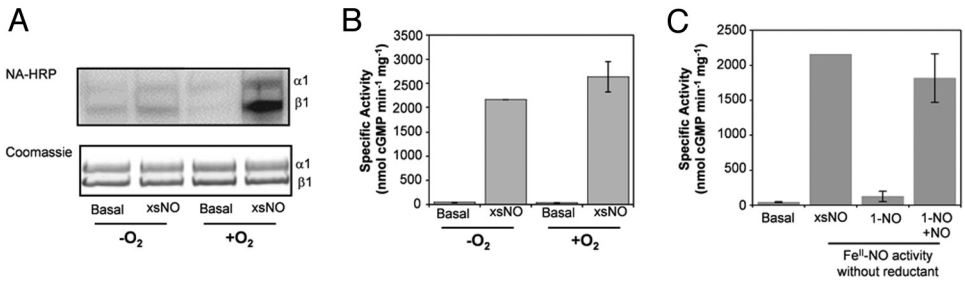

Fig. 3. The effect of redox active reagents on NO-stimulated sGC activity. (*A*) The biotin-switch method shows that cysteines on the α1 and β1 subunits are only S-nitrosated in the presence of both NO and O_2. (*B*) sGC activity was examined in the presence and absence of O_2. (*C*) The sGC Fe^{II}-NO complex was formed with excess NO (xsNO) in the absence of reducing agent. Excess NO was removed from the Fe^{II}-NO complex (1-NO) and the sample was retreated with excess NO (1-NO + NO). All experiments were performed in the absence of reducing agent. Data are presented as means ± SD.

enzyme activation is likely the same under anaerobic and aerobic conditions. Thus, the observation of maximal NO stimulation of sGC without S-nitrosation excludes a nitrosothiol as the cysteine modification involved in sGC activation by NO.

The observation of maximal NO stimulation with S-nitrosation under aerobic conditions presents an apparent discrepancy with literature reports that S-nitrosation of specific sGC cysteines (β1C122 and α1C243) inhibits sGC activity (19). This discrepancy can be reconciled by noting the difference in assay conditions between the work reported here and the previously published report. The experiments presented here were designed to study the molecular events of NO stimulation of sGC and, accordingly, a short reaction with the NO donor DEA/NO was used. However, the experiments that identified an inhibitory action of S-nitrosation were designed to simulate conditions of physiological NO tolerance; therefore a relatively long reaction with *S*-nitrosoglutathione (GSNO) was used (19). Furthermore, GSNO acts primarily through transnitrosation whereas the mechanism of S-nitrosation by NO typically proceeds through the reaction with O_2. Because of the difference in nitrosating reagents and reaction conditions, different cysteine residues will react to different extents in each experiment. Therefore, although our data eliminates a role for a nitrosothiol in the activation of sGC, it does not conflict with the proposal that S-nitrosation is involved in the mechanism of NO tolerance (19, 26, 27).

To further explore the role of redox chemistry in the NO/cysteine interaction, the reversibility of sGC activity in the absence of commonly used redox reactive reagents, such as O_2 and DTT was studied. As discussed above, sGC can be fully activated by NO in the absence of O_2 and DTT (Fig. 3*B*). If NO activation was caused by an NO-induced oxidation, NO stimulation would not be reversible without a reductant. To assess the reversibility of this reaction anaerobically, the xsNO species was formed and then excess NO was removed from solution to form the low-activity 1-NO species (Fig. 3*C*). The activity of both the xsNO and 1-NO species with or without O_2 and DTT is similar (Figs. 1*D* and 3*C*). The 1-NO sGC species was then restimulated with NO, and the enzyme regained full activation (1-NO + NO in Fig. 3*C*). Thus, just as activation by NO did not require an oxidation of sGC, deactivation and restimulation did not require a reduction of sGC. Because sGC activation is rapidly reversible in the absence of redox mediators, we conclude that the activating species does not alter the oxidation state of the key cysteine(s). Furthermore, because the level of activity of each sGC state is unaffected by anaerobic conditions, we propose that the mechanism of activation and deactivation is O_2-independent. Additionally, the necessity for a reduced thiol in the non-heme NO binding site provides a specific mechanism for the inhibition of NO stimulated activity by thiol oxidation (17, 18, 20) and S-nitrosation (19, 26). A chemical species that could account for these observations is the direct nucleophilic addition of a thiol to NO, which yields $RSNO^{\cdot-}$. This species differs from a nitrosothiol by only one electron, but this small difference imparts radically different properties. As opposed to the relative stability of nitrosothiols, this species has been proposed as a short-lived intermediate in reactions that yield disulfides, sulfenic acids, and nitrosothiols (28–30) and has been characterized as a reversible adduct on hemoglobin (31). The characteristic of rapid reversibility is consistent with the rapid deactivation of sGC from the xsNO state to the 1-NO state.

Investigation of cGMP Regulation by NO in HUVECs. Decades of in vitro experiments have established that sGC activation requires the coordination of NO to the heme; however, a NO-bound species has not been directly observed in vivo. Spectroscopy is the standard method of detection for the ligation state of a hemoprotein (32), but the complexity of cellular constituents

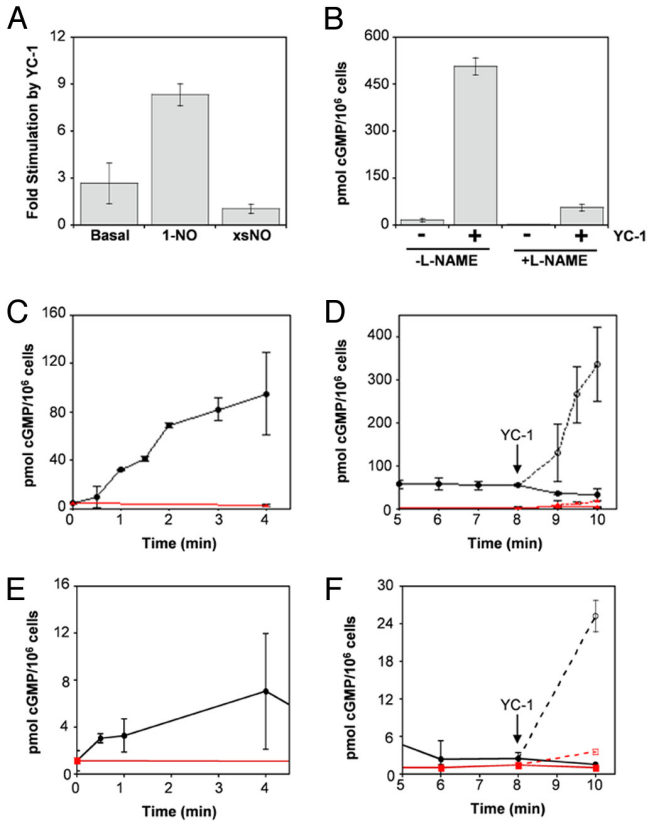

Fig. 4. Characterization of three different sGC states in HUVECs. (*A*) Fold activation induced by YC-1 of the basal, 1-NO, and xsNO states of purified sGC. (*B*) YC-1 activation of HUVECs in the absence and presence of L-NAME. (*C–F*) Time course of cGMP levels in HUVECS in the presence (*C* and *D*) and absence (*E* and *F*) of IBMX. Plots display both the early (*C* and *E*) and late (*D* and *F*) phases with (black) and without (red) 1 μM PROLI/NO addition at 0 min. Basal (red closed squares) and NO-stimulated (black closed circles) cells are shown before and after 150 μM YC-1 addition at 8 min, as indicated by an arrow. YC-1 treatment at 8 min significantly activates the cells that had been exposed to NO at 0 min (open black circles) but not the control cells (open red circles). Data are presented as means ± SD.

and the low abundance of sGC in vivo severely limit the utility of spectroscopy in cells. Therefore, to observe the sGC heme coordination state in vivo, we have used an alternative assay that capitalizes on the small molecule sGC activator YC-1 (22). YC-1 activates sGC to different degrees depending on the heme ligation state (21, 33). Although the precise mechanism of YC-1 activation is still under investigation, YC-1 can be used to distinguish sGC heme ligation states by the differential activation of the 1-NO state compared with the basal state or the xsNO state (Fig. 4*A*) (7).

To assess the heme ligation state of sGC in vivo, cGMP formation in human umbilical vein endothelial cells (HUVECs) was examined. These cells constitutively express both sGC and NO synthase (NOS) and exhibit a low level of basal cGMP. Upon YC-1 treatment of HUVECs, a large increase in cGMP formation was observed. This YC-1-dependent increase in cGMP levels was prevented by a 2-h preincubation with N^{ω}-nitro-L-arginine methyl ester (L-NAME), a cell permeable NOS inhibitor (Fig. 4*B*). This demonstrates a requirement for NO in the YC-1 mediated activation of sGC in vivo and others have observed similar phenomena in porcine aortic endothelial cells (PAECs) (34), implicating a generality of this property in endothelial cells. Both the high fold activation of cGMP production induced by YC-1 and the inhibition of this activation by

Table 3. YC-1 stimulation of multiple sGC states in HUVECs

NO treatment	YC-1	Phase	Velocity, pmol/min/10^6 cells
None	−	Early	0*
	+	Early	ND
None	−	Late	0*
	+	Late	8.79 ± 1.60
1 μM	−	Early	32.28 ± 12.83
	+	Early	96.92 ± 32.03
1 μM	−	Late	0*
	+	Late	125.45 ± 46.69

HUVEC rates acquired at 37 °C. For NO treatment, addition of 1 μM PROLI/NO at $t = 0$ min. Early phase is between 0 and 3 min and late phase is between 5 and 10 min. Velocity was determined by global analysis of mean measurements. ND, not determined. *, Velocity not statistically different from zero.

an extended pretreatment with L-NAME are consistent with the 1-NO state, however, the uncertainty of the local concentration of NO complicates this interpretation.

The kinetics of NO stimulation in vivo have been studied extensively (35, 36). In response to NO, cells expressing sGC exhibit a rapid elevation in intracellular cGMP levels, followed by a fast decline in the rate of cGMP synthesis. This rapid deactivation has been previously assumed to reflect the simple dissociation of NO from the sGC heme. This would limit sGC to two defined states: an active NO-bound state and a basal NO-free state. However, experiments with purified protein suggest that the high activity, xsNO state may deactivate to the 1-NO state rather than the basal state (7). This possibility was tested in a cellular context with a time course assay in L-NAME-treated HUVECs that were exposed to a burst of NO (delivered by PROLI/NO) in the presence of a phosphodiesterase (PDE) inhibitor (3-isobutyl-1- methylxanthine, IBMX). The sGC activity was then measured in both the early phase of NO stimulation (0–4 min) (Fig. 4*C*) and the late phase of NO stimulation (5–10 min) (Fig. 4*D*) (Table 3). In the early phase, HUVECs displayed a well-documented accumulation of cGMP in response to NO, whereas untreated control HUVECs maintained a low, basal level of cGMP (≈1 pmol/10^6 cells) (Fig. 4*C*). This accounts for the two well-established states of sGC; the low activity of the basal state and the high activity of the xsNO state. In the late phase, the intracellular cGMP level reached a plateau indicative of the deactivated, low-activity sGC state (Fig. 4*D*). In the late phase, both NO stimulated and untreated HUVECs exhibited low sGC activity which has been assumed to be the activity of basal sGC, i.e., no ligand bound to the heme. However, YC-1 treatment only stimulates sGC activity in the NO-treated cells, and the specific and prominent activation of only these cells discriminates between two long-lived, low-activity species with differing propensities toward YC-1 in vivo.

To simplify data analysis, the experiments described above were performed in the presence of a PDE inhibitor; however, in vivo PDEs are intimately linked to cGMP signaling and shape temporal changes in NO-induced intracellular cGMP levels (37). Therefore, similar experiments were performed in the absence of IBMX, where we found that PDE activity did not affect the cellular responses under investigation (Fig. 4 *E* and *F*). Importantly, under the conditions of this experiment, NO rapidly decays such that none was detected in solution after 4 min (Fig. S4), eliminating the uncertainty in local NO concentration.

These experiments suggest that sGC exists in three states in vivo: a low-activity state that is weakly stimulated by YC-1 (basal), a short-lived, high-activity state that is weakly stimulated by YC-1 (xsNO), and a longer-lived, low-activity state that is highly stimulated by YC-1 (Table 3). Because this closely mirrors the activities of the spectroscopically defined states of sGC in vitro, this would appear to be a clear observation of the 1-NO state in vivo. With this evidence we propose a model of sGC activation where a reduced cysteine(s) stabilizes NO binding and produces a highly active sGC state (Fig. 5). The rapid dissociation of the cysteine/NO complex deactivates the enzyme to the 1-NO state, which persists until NO slowly dissociates from the sGC heme and the enzyme reverts to the basal state.

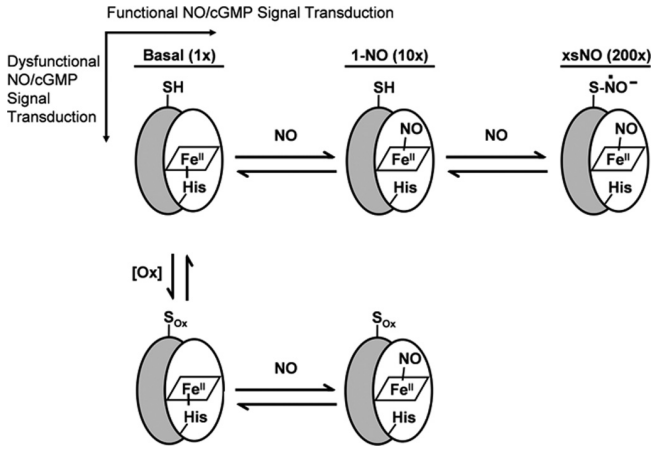

Fig. 5. Model for the role of cysteine(s) in the mechanism of sGC activation. NO initially binds to the heme and activates the enzyme ≈10-fold. In the presence of excess NO (xsNO), a putative thiol-NO adduct forms and this activates the enzyme ≈200-fold above the basal level. Although the exact chemical identity is unknown, a thionitroxide is proposed. This species is consistent with the observed properties of activation and deactivation. Under oxidative stress, the non-heme NO binding site oxidizes which prevents NO binding and, therefore, maximal activation. For simplicity, oxidation is only shown to affect the basal state, however, oxidation of the non-heme NO binding site in any state would desensitize sGC to NO.

Conclusion

In summary, our findings establish the importance of an sGC cysteine in the regulation of sGC by NO (Fig. 5). Multiple NO binding sites impart a complexity of regulation to sGC which could be useful for the NO/cGMP signal transduction pathway because it intersects a great variety of physiological processes. It is noteworthy that both sites of NO interaction on sGC, a reduced thiol and a ferrous iron, are susceptible to oxidation. Therefore, in physiological instances of oxidative stress, it is possible that both cysteine oxidation and heme oxidation contribute to sGC dysfunction by preventing NO binding to each respective site. The interplay between these multiple sGC states and the molecular causes of dysfunction may offer an opportunity for the design of state-specific sGC activators to target diseased tissue (38, 39).

Materials and Methods

sGC in Vitro Assays. Recombinant rat sGC was purified as described in ref. 14 and then DTT was removed from the sGC storage buffer using an anion exchange column. sGC was assayed in the presence and absence of MMTS (50 μM), PROLI/NO (50 μM) and YC-1 (150 μM) where indicated, at room temperature. Assays were initiated with substrate, quenched after 3 min and cGMP was quantified. MMTS inhibition of sGC was directly compared with sGC activation by 1 equivalent of NO. sGC with NO only at the heme was formed by addition of substoichiometric amounts of PROLI/NO and spectrally monitoring the formation of the sGC-NO complex. Samples (sGC and sGC-NO) were then incubated with MMTS (30 μM) and assays were initiated by addition of substrate at room temperature. Samples were quenched after 3 min and cGMP was quantified. Reversibility of MMTS inhibition was examined by adding DTT (5 mM) to MMTS-treated sGC, and quantifying cGMP production. To determine the inhibition profile of MMTS on NO-stimulated activity the concentration of MMTS was varied from 0 to 100 μM. All assays were initiated by addition of $MgCl_2$ (3 mM) and GTP (1.5 mM) and cGMP was quantified. All

statistic results are given as means ± SD, and significance was evaluated using unpaired *t* tests (Microsoft).

Effect of Oxidants on sGC Activity. The effect of redox active reagents on sGC activity was investigated. The reversibility of NO activation in the absence of DTT was examined by treating sGC with PROLI/NO followed by desalting into a NO-free and DTT-free buffer. The NO-bound enzyme was then assayed in the absence and presence of PROLI/NO (50 μM) at room temperature. The protein was examined with activity assays and electronic absorption spectroscopy after each manipulation. NO-stimulated activity was also examined in the presence and absence of O_2 (44 μM) in a DTT-free buffer at 37 °C. Assays were initiated with $MgCl_2$ (3 mM) and GTP (1.5 mM), quenched after 3 min, and cGMP was analyzed.

Cysteine S-nitrosation in the presence and absence of O_2 and NO was examined by the biotin-switch method (40) with minor modification. This method specifically replaces a nitrosothiol with a biotin tag by selectively reducing nitrosothiols with ascorbate, and then labeling newly formed thiols with a biotin moiety. The reactions were analyzed by Coomassie blue staining and Neutravidin-HRP Western blot. With this method biotinylation is a marker for S-nitrosation.

MMTS Labeling of sGC. To visualize MMTS labeling of sGC a method was developed based on existing protocols (40, 41). Briefly, free thiols were blocked with *N*-ethylmaleimide (NEM) and then DTT was used to reduce disulfides. Free thiols were then specifically labeled with biotin. These samples were evaluated by SDS/PAGE with Coomassie staining or Western blot analysis using a Neutravidin-HRP conjugate. In these experiments, biotinylation is a marker for the MMTS-thiol reaction product.

PC12 Activity Assays. Semiadherent PC12 cells (ATCC) were maintained in DMEM (Invitrogen) supplemented with 10% FBS according to the manufacturer's instructions. Cells were washed extensively with ice-cold assay buffer [50 mM Hepes (pH 7.4), 50 mM NaCl] and then incubated with MMTS (0–300 μM) on ice for 10 min. Reactions were initiated by addition of PROLI/NO (1 μM) at 37 °C. After 5 seconds, reactions were quenched with HCl, and total protein and cGMP concentrations were quantified.

HUVEC Activity Assays. HUVECs were grown to confluence in EGM-2 media supplemented by bullet kit according to distributor's instructions (Lonza). Cells were then incubated with or without L-NAME (300 μM) for 2 h. After pretreatment, media were replaced with 50 mM Hepes (pH 7.4), 100 mM NaCl, 5 mM KCl, 2.5 mM $CaCl_2$, 1 mM $MgCl_2$, 1 mM IBMX and, where indicated, 300 μM L-NAME. Samples were incubated for 15 min and then reactions were initiated by addition of PROLI/NO (1 μM) and/or YC-1 (150 μM). End-point assays proceeded for 4 min, whereas time course kinetics proceeded for the indicated duration at 37 °C. Reactions were terminated by addition of HCl and cGMP was quantified. All statistic results are given as means ± SD, and significance was evaluated using unpaired *t* tests.

Detailed methods can be found in the *SI Text*.

ACKNOWLEDGMENTS. We thank Dr. Arnie Falick, Dr. David King, Dr. Tony Iavarone, and Dr. Lori Kohlstaedt for MS help and advice; Dr. Stephen Cary and Dr. Jonathan Winger for critical input; Dr. Joshua Woodward for helpful discussions; Sarah Deng for technical assistance; and Dr. Arnie Falick (University of California, Berkeley) for acquiring the MALDI-TOF/TOF spectra. This study was funded by National Institutes of Health Grant GM077365 (to M.A.M.).

1. Munzel T, et al. (2003) Physiology and pathophysiology of vascular signaling controlled by guanosine 3′,5′-cyclic monophosphate-dependent protein kinase. *Circulation* 108:2172–2183.
2. Sanders KM, *et al*. (1992) Nitric-oxide as a nonadrenergic, noncholinergic neurotransmitter in the gastrointestinal-tract. *Jpn J Pharmacol* 58:220–225.
3. Warner TD, Mitchell JA, Sheng H, Murad F (1994) Effects of cyclic GMP on smooth muscle relaxation. *Adv Pharmacol* 26:171–194.
4. Arnold WP, Mittal CK, Katsuki S, Murad F (1977) Nitric-oxide activates guanylate cyclase and increases guanosine 3′-5′-cyclic monophosphate levels in various tissue preparations. *Proc Natl Acad Sci USA* 74:3203–3207.
5. Gerzer R, Hofmann F, Schultz G (1981) Purification of a soluble, sodium-nitroprusside-stimulated guanylate-cyclase from bovine lung. *Eur J Biochem* 116:479–486.
6. Wolin MS, Wood KS, Ignarro LJ (1982) Guanylate-cyclase from bovine lung: A kinetic-analysis of the regulation of the purified soluble enzyme by protoporphyrin-IX, heme, and nitrosyl-heme. *J Biol Chem* 257:3312–3320.
7. Cary SP, Winger JA, Marletta MA (2005) Tonic and acute nitric oxide signaling through soluble guanylate cyclase is mediated by nonheme nitric oxide, ATP, and GTP. *Proc Natl Acad Sci USA* 102:13064–13069.
8. Russwurm M, Koesling D (2004) NO activation of guanylyl cyclase. *EMBO J* 23:4443–4450.
9. Stone JR, Marletta MA (1996) Spectral and kinetic studies on the activation of soluble guanylate cyclase by nitric oxide. *Biochemistry* 35:1093–1099.
10. Zhao Y, Brandish PE, Ballou DP, Marletta MA (1999) A molecular basis for nitric oxide sensing by soluble guanylate cyclase. *Proc Natl Acad Sci USA* 96:14753–14758.
11. Kharitonov VG, Russwurm M, Magde D, Sharma VS, Koesling D (1997) Dissociation of nitric oxide from soluble guanylate cyclase. *Biochem Biophys Res Commun* 239:284–286.
12. Winger JA, Derbyshire ER, Marletta MA (2006) Dissociation of nitric oxide from soluble guanylate cyclase and H-NOX domain constructs. *J Biol Chem* 282:897–907.
13. Derbyshire ER, *et al*. (2008) Characterization of two different five-coordinate soluble guanylate cyclase ferrous-nitrosyl complexes. *Biochemistry* 47:3892–3899.
14. Derbyshire ER, Marletta MA (2007) Butyl isocyanide as a probe of the activation mechanism of soluble guanylate cyclase: Investigating the role of non-heme nitric oxide. *J Biol Chem* 282:35741–35748.
15. Aono S (2008) Metal-containing sensor proteins sensing diatomic gas molecules. *Dalton Trans* 3137–3146.
16. Chen L, Lyubimov AY, Brammer L, Vrielink A, Sampson NS (2008) The binding and release of oxygen and hydrogen peroxide are directed by a hydrophobic tunnel in cholesterol oxidase. *Biochemistry* 47:5368–5377.
17. Brandwein HJ, Lewicki JA, Murad F (1981) Reversible inactivation of guanylate-cyclase by mixed disulfide formation. *J Biol Chem* 256:2958–2962.
18. Braughler JM (1983) Soluble guanylate cyclase activation by nitric oxide and its reversal. Involvement of sulfhydryl group oxidation and reduction. *Biochem Pharmacol* 32:811–818.
19. Sayed N, Baskaran P, Ma X, van den Akker F, Beuve A (2007) Desensitization of soluble guanylyl cyclase, the NO receptor, by S-nitrosylation. *Proc Natl Acad Sci USA* 104:12312–12317.
20. Maron BA, *et al*. (2009) Aldosterone increases oxidant stress to impair guanylyl cyclase activity by cysteinyl thiol oxidation in vascular smooth muscle cells. *J Biol Chem* 284:7665–7672.
21. Friebe A, Schultz G, Koesling D (1996) Sensitizing soluble guanylyl cyclase to become a highly CO-sensitive enzyme. *EMBO J* 15:6863–6868.
22. Ko FN, Wu CC, Kuo SC, Lee FY, Teng CM (1994) YC-1, a novel activator of platelet guanylate cyclase. *Blood* 84:4226–4233.
23. Bal-Price A, Gartlon J, Brown GC (2006) Nitric oxide stimulates PC12 cell proliferation via cGMP and inhibits at higher concentrations mainly via energy depletion. *Nitric Oxide* 14:238–246.
24. Boerrigter G, Burnett JC (2007) Nitric oxide-independent stimulation of soluble guanylate cyclase with BAY 41–2272 in cardiovascular disease. *Cardiovasc Drug Rev* 25:30–45.
25. Hess DT, Matsumoto A, Kim SO, Marshall HE, Stamler JS (2005) Protein S-nitrosylation: Purview and parameters. *Nat Rev Mol Cell Bio* 6:150–166.
26. Mayer B, *et al*. (2009) Inactivation of soluble guanylate cyclase by stoichiometric S-nitrosation. *Mol Pharmacol* 75:886–891.
27. Sayed N, *et al*. (2008) Nitroglycerin-induced S-nitrosylation and desensitization of soluble guanylyl cyclase contribute to nitrate tolerance. *Circ Res* 103:606–614.
28. DeMaster EG, Quast BJ, Redfern B, Nagasawa HT (1995) Reaction of nitric oxide with the free sulfhydryl group of human serum albumin yields a sulfenic acid and nitrous oxide. *Biochemistry* 34:11494–11499.
29. Gow AJ, Buerk DG, Ischiropoulos H (1997) A novel reaction mechanism for the formation of S-nitrosothiol in vivo. *J Biol Chem* 272:2841–2845.
30. Pryor WA, Church DF, Govindan CK, Crank G (1982) Oxidation of thiols by nitric-oxide and nitrogen-dioxide - synthetic utility and toxicological implications. *J Org Chem* 47:156–159.
31. Zhao YL, Houk KN (2006) Thionitroxides, RSNHO center dot: The structure of the SNO moiety in ''S-nitrosohemoglobin'', a possible NO reservoir and transporter. *J Am Chem Soc* 128:1422–1423.
32. Antonini E, Brunori M (1971) *Hemoglobin and Myoglobin in Their Reactions with Ligands* (North-Holland, Amsterdam).
33. Martin E, Lee YC, Murad F (2001) YC-1 activation of human soluble guanylyl cyclase has both heme-dependent and heme-independent components. *Proc Natl Acad Sci USA* 98:12938–12942.
34. Schmidt K, Schrammel A, Koesling D, Mayer B (2001) Molecular mechanisms involved in the synergistic activation of soluble guanylyl cyclase by YC-1 and nitric oxide in endothelial cells. *Mol Pharmacol* 59:220–224.
35. Bellamy TC, Garthwaite J (2002) Pharmacology of the nitric oxide receptor, soluble guanylyl cyclase, in cerebellar cells. *Brit J Pharmacol* 136:95–103.
36. Roy B, Garthwaite J (2006) Nitric oxide activation of guanylyl cyclase in cells revisited. *Proc Natl Acad Sci USA* 103:12185–12190.
37. Soderling SH, Beavo JA (2000) Regulation of cAMP and cGMP signaling: New phosphodiesterases and new functions. *Curr Opin Cell Biol* 12:174–179.
38. Boerrigter G, *et al*. (2007) Targeting heme-oxidized soluble guanylate cyclase in experimental heart failure. *Hypertension* 49:1128–1133.
39. Stasch JP, *et al*. (2006) Targeting the heme-oxidized nitric oxide receptor for selective vasodilatation of diseased blood vessels. *J Clin Invest* 116:2552–2561.
40. Jaffrey SR, Snyder SH (2001) The biotin switch method for the detection of S-nitrosylated proteins. *Science STKE* 2001:PL1.
41. Leichert LI, Jakob U (2006) Global methods to monitor the thiol-disulfide state of proteins in vivo. *Antioxid Redox Signal* 8:763–772.

Supporting Information

Fernhoff et al. 10.1073/pnas.0911083106

SI Text

Cell Culture. Pooled human umbilical vascular endothelial cells (HUVECs) were obtained from Lonza and maintained in EGM-2 media supplemented with a bulletkit (Lonza) according to the manufacturer's instructions. Semiadherent PC12 cells were obtained from the American Type Culture Collection and maintained in a humidified atmosphere of 95% air and 5% CO_2 at 37 °C in DMEM (Invitrogen) supplemented with 10% FBS, L-glutamine (200 μg/mL), penicillin (100 U/mL), and streptomycin (100 μg/mL). Cells were counted with a hemocytometer and viability was routinely assessed by trypan blue staining and found to be >90%.

HUVEC Activity Assays. Confluent HUVECs in either 6-well plates or 100 × 15 mm Petri dishes were preincubated, where indicated, with 300 μM L-NAME in growth media for 2 h. After pretreatment, media were replaced with 50 mM Hepes (pH 7.4), 100 mM NaCl, 5 mM KCl, 2.5 mM $CaCl_2$, 1 mM $MgCl_2$, 1 mM IBMX and, where indicated, 300 μM L-NAME. Samples were incubated for 15 min, and then reactions were initiated with additions of 1 μM PROLI/NO (Cayman Chemicals) and/or 150 μM YC-1 (Sigma). End-point assays proceeded for 4 min, whereas time course kinetics proceeded for the indicated duration. Reactions were terminated by aspiration of the assay buffer and immediate addition of 100 mM HCl. Quenched reactions were incubated at 4 °C for 30 min, scraped with a rubber policeman, transferred to a 1.5-mL Eppendorf tube, and stored at −80 °C until cGMP quantification was carried out using a cGMP enzyme immunoassay kit, Format A (Assay Designs), per the manufacturer's instructions. All manipulations before quenching were performed at 37 °C and HUVECs used for cGMP measurements were between passages 3–10. Each assay point was done in duplicate or triplicate and all experiments were repeated 3–4 times to ensure reproducibility.

sGC in Vitro Assays. sGC was purified as described in ref. 1. MMTS inhibition of sGC was directly compared with sGC activation by 1 equivalent of NO. In all experiments, MMTS (Pierce) was prepared fresh in assay buffer before each assay. sGC with NO only at the heme was formed by addition of substoichiometric amounts of PROLI/NO and monitored spectrally for the formation of the sGC-NO complex. Samples (sGC and sGC-NO) were then incubated with MMTS (30 μM) for 30 min on ice. Duplicate end-point assays were initiated by addition of 3 mM $MgCl_2$ and 1.5 mM GTP at 25 °C. Samples were quenched after 3 min by the addition of 400 μl of 125 mM $Zn(CH_3CO_2)_2$ and 500 μl of 125 mM Na_2CO_3. cGMP was quantified using a cGMP enzyme immunoassay kit, Format B (Biomol), per the manufacturer's instructions. All experiments were repeated 3–4 times to ensure reproducibility.

sGC activity was measured in the presence of MMTS. sGC (22 nM) was incubated with 13 μM MMTS in 50 mM Hepes (pH 7.4), 50 mM NaCl on ice for 60 min. Samples were then incubated in the presence or absence of 5 mM DTT for an additional 60 min on ice. sGC activity was measured in duplicate in the presence and absence of DEA/NO (100 μM) and YC-1 (150 μM) by addition of 3 mM $MgCl_2$ and 1.5 mM GTP at 25 °C.

To determine the inhibition profile of MMTS on NO-stimulated activity, the concentration of MMTS was varied from 0 to 100 μM. In these experiments, sGC (133 nM) was incubated with MMTS at the indicated concentration for 5 min at 25 °C before a 10-fold dilution and DEA/NO (50 μM) addition. Duplicate 3 min end-point assays were initiated with 3 mM $MgCl_2$ and 1.5 mM GTP at 25 °C. Data analysis and figure generation were carried out using Kaleidagraph (Synergy Software). All statistic results are given as means ± SD, and significance was evaluated using unpaired *t* tests (Microsoft).

MMTS Labeling of sGC. To visualize MMTS labeling of sGC the following method was developed based on existing protocols (2, 3). Specifically, after sGC was incubated with MMTS, reactions were quenched with 1 equivalent of 250 mM Hepes (pH 7.2), 1 mM EDTA, 0.1 mM neocuproine, 10% SDS, 80 mM NEM for 30 min at 65 °C. Samples were acetone precipitated and protein pellets were then resuspended in 62 mM Hepes (pH 7.2), 0.25 mM, EDTA, 0.025 mM neocuproine, 5% SDS, 20 mM DTT and incubated at 37 °C for 30 min. Samples were again acetone precipitated and then resuspended in 62 mM Hepes (pH 7.2), 0.25 mM EDTA, 0.025 mM neocuproine, 5% SDS, 5 mM maleimide-PEO_2-biotin (Pierce) and incubated for 1 h at 37 °C. This reaction was quenched by addition of 50 mM DTT and SDS/PAGE loading buffer, and the samples were split and evaluated by SDS/PAGE using precast 10% Tris-glycine gels (Invitrogen). One gel was stained with Coomassie to control for loading whereas another gel was transferred to nitrocellulose, stained with a Neutravidin-HRP conjugate (Pierce), and imaged with West Femto imaging solutions (Pierce) on a FluorS imaging station (Bio-Rad). Densitometry analysis was carried out with QuantityOne software (Bio-Rad).

Peptide Mapping. MMTS-treated sGC (15 μg) was blocked with 40 mM NEM and acetone precipitated. The protein pellet was resuspended in 10 μl of 50 mM Hepes (pH 7.2), 20 mM NEM, 6 M guanidinium HCl and heated to 55 °C for 30 min. The reaction was diluted 10-fold with 50 mM Tris (pH 7.6), 1 mM $CaCl_2$, and then 150 ng of Trypsin Gold (Promega) was added. Digests proceeded for 12 h at 37 °C and were concentrated by Speed Vac to ≈30 μl. Samples were then prepared for either mudPIT or MALDI-TOF/TOF.

MudPIT analysis was performed by the Proteomics/Mass Spectrometry Laboratory at the University of California Berkeley. Sample was first desalted using a C18 spec tip (Varian). A nano LC column was packed in a 100-μm inner diameter glass capillary with an emitter tip. The column consisted of 10 cm of Polaris C18 (5 μm) packing material (Varian), followed by 4 cm of PartiSphere 5 SCX (Whatman). The column was loaded by use of a pressure bomb and washed extensively with buffer A (4). The column was then directly coupled to an electrospray ionization source mounted on a Thermo–Fisher LTQ XL linear ion trap mass spectrometer. An Agilent 1200 HPLC equipped with a split line to deliver a flow rate of 30 nl/min was used for chromatography. Peptides were eluted using a 4-step MudPIT procedure (4). The program DTASelect was used to identify modified peptides from the rat sGC sequence.

For MALDI-TOF/TOF, peptides from the digest solution were adsorbed onto a C18 ZipTip and eluted with 5 μl of 60% acetonitrile/ 0.5% TFA saturated with HCCA. Samples were spotted and allowed to dry on the MALDI target. A fullscan mass spectrum of the digest was recorded on an Applied Biosystems 4800 MALDI tandem TOF instrument in reflector mode. The ions at *m/z* corresponding to protonated modified peptides were then isolated in MS1, and individual CID spectra were acquired with air used as the collision gas at 1.0 keV collision energy.

Effect of S-Nitrosation on sGC Activity. sGC activity and nitrosothiol formation were monitored in the presence and absence of O_2 to determine whether S-nitrosation activates sGC. In an anaerobic chamber (Coy), residual DTT was removed from sGC by two cycles of dilution/concentration using a 10K Ultrafree-0.5 centrifugal filter device (Vivaspin). sGC (0.2 μg) was then assayed in the presence and absence of 40 μM DEA/NO in duplicate at 37 °C. This set of assays was done both in the absence and presence of O_2 (237 μM). Assay mixtures contained 50 mM Hepes (pH 7.4), 50 mM NaCl, 3 mM $MgCl_2$, 1.5 mM GTP and were in a final volume of 100 μl. Assays were quenched after 3 min and analyzed as described above. To evaluate cysteine S-nitrosation, identically prepared sGC samples were examined by the biotin-switch method (2) with minor modification. Briefly, S-nitrosation was allowed to proceed for 5 min, and reactions were then quenched aerobically with an equal volume of 250 mM Hepes (pH 7.2), 1 mM EDTA, 0.1 mM neocuproine, 10% SDS, 120 mM NEM. Reactions were transferred to 65 °C for 30 min and vortexed frequently. Samples were then acetone precipitated and the protein pellets were subsequently dissolved in 30 μl of 62 mM Hepes (pH 7.2), 0.25 mM EDTA, 0.025 mM neocuproine, 5% SDS, 1 mM maleimide-PEO_2-biotin (Pierce), 10 mM sodium ascorbate, and incubated for 1 h at 25 °C. The reactions were quenched by addition of SDS/PAGE loading buffer containing 50 mM DTT. The samples were then split and analyzed by both Coomassie blue staining and Neutravidin-HRP Western blot, as described above. The total protein loaded into each well was 2.6 μg for the biotin-switch method and 1.3 μg for the Coomassie gel.

PC12 Cells Activity Assays. Semiadherent PC12 cells in 150 × 15 mm Petri dishes were washed extensively with ice-cold assay buffer [50 mM Hepes (pH 7.4), 50 mM NaCl] and harvested with a rubber policeman. Cells were collected by centrifugation at 4 °C and gently resuspended in ice-cold assay buffer. Cells were then incubated with MMTS (0–300 μM) on ice for 10 min. Reactions were then transferred to 37 °C for 10 seconds before addition of 1 μM PROLI/NO. After 5 seconds, reactions were quenched with 1 volume of 133 mM HCl. Protein concentration was measured in each sample using the Bradford Microassay (Bio-Rad) against a BSA standard, and cGMP quantification was carried out using a cGMP enzyme immunoassay kit, Format A (Assay Designs), per the manufacturer's instructions. Each assay point was done in duplicate and all experiments were repeated 3–4 times to ensure reproducibility. Data analysis and figure generation were carried out using Kaleidagraph (Synergy Software). All statistic results are given as means ± SD, and significance was evaluated using unpaired *t* tests (Microsoft).

Direct Detection of Solution NO. The concentration of NO in solution was quantified after addition of PROLI/NO at various times points. A solution of 50 mM Hepes (pH 7.4), 100 mM NaCl, 5 mM KCl, 2.5 mM $CaCl_2$, 1 mM $MgCl_2$ (1 mL total volume) was deposited in a 6-well plate at 37 °C. NO decomposition was initiated by addition of 1 μM PROLI/NO to the solution. At the indicated times, aliquots (200 μl) were withdrawn and immediately sealed in a 1.25 mL reacti-vial. After vortexing the vial, 5 mL of headspace was removed with a gas-tight Hamilton syringe and injected into a Sievers Nitric Oxide Analyzer NOA 280i. The NO detection limit of the NOA is ≈1 ppb. Peak area was quantified with the manufacturer's software. Data shown is the average of eight independent trials.

1. Derbyshire ER, Marletta MA (2007) Butyl isocyanide as a probe of the activation mechanism of soluble guanylate cyclase: Investigating the role of non-heme nitric oxide. *J Biol Chem* 282:35741–35748.
2. Jaffrey SR, Snyder SH (2001) The biotin switch method for the detection of *S*-nitrosylated proteins. *Science STKE* 2001:PL1.
3. Leichert LI, Jakob U (2006) Global methods to monitor the thiol-disulfide state of proteins in vivo. *Antioxid Redox Signal* 8:763–772.
4. Washburn MP, Wolters D, Yates JR, 3rd (2001) Large-scale analysis of the yeast proteome by multidimensional protein identification technology. *Nat Biotechnol* 19:242–247.

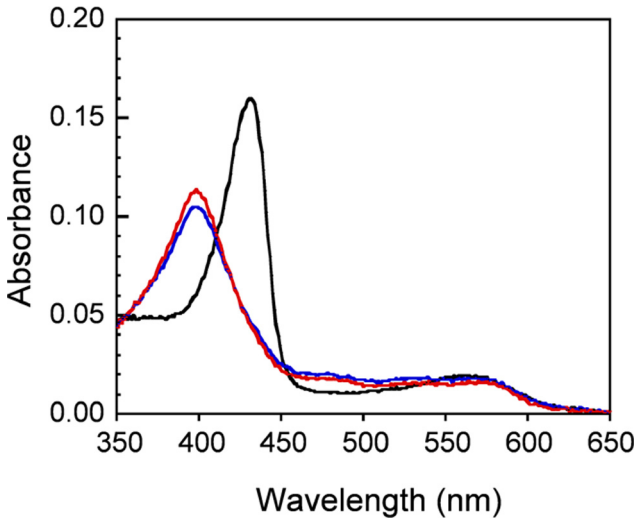

Fig. S1. Electronic absorption spectra of the sGC-NO complex in the absence and presence of MMTS. Ferrous unligated sGC (black line) was treated with 30 μM MMTS and then exposed to 50 μM PROLI/NO (blue line). The MMTS-treated protein forms a ferrous-nitrosyl complex that is identical to the spectrum of the ferrous-nitrosyl complex formed in the absence of MMTS (red line).

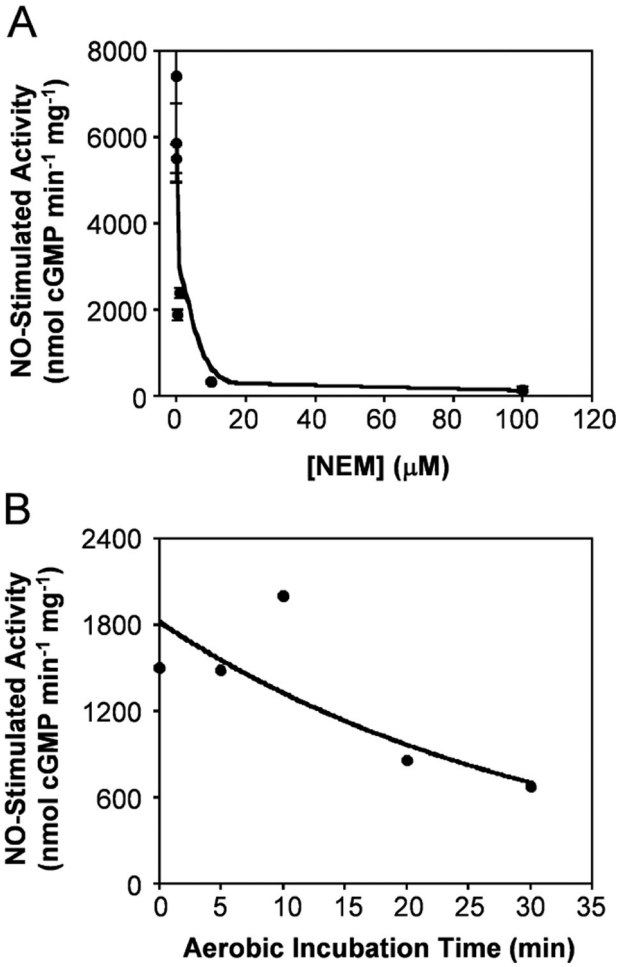

Fig. S2. Inhibition of NO-stimulated sGC by thiol modification and oxidation. (*A*) Titration of NEM against NO-stimulated sGC activity shows NEM inhibition saturates at a level that is greater than basal sGC activity. (*B*) NO-stimulated sGC activity decreases when the enzyme is incubated in the absence of DTT in an aerobic buffer at 25 °C.

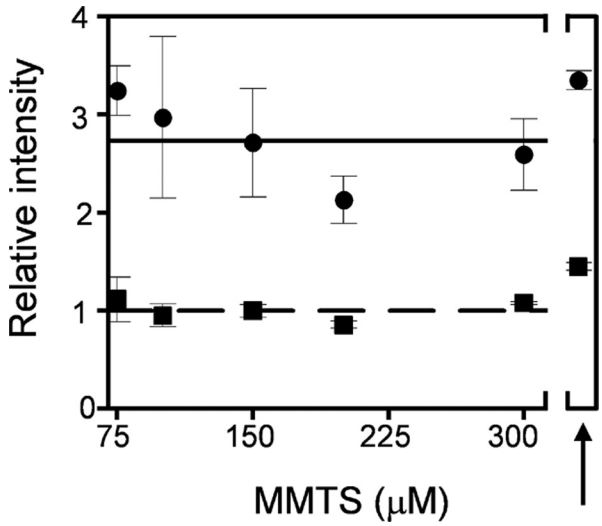

Fig. S3. MMTS labeling of sGC. At high MMTS concentrations, the labeling observed on the α1 subunit (circles) and the β1 subunit (squares) saturates. This level of saturation is below the intensity observed when denatured protein reacts with excess MMTS (arrow). Densitometry analysis estimates the maximum number of cysteines that can react with MMTS in the folded protein to be 16 $\pm$ 3 cysteines on α1 and 10 $\pm$ 1 cysteines on β1. Data are presented as means $\pm$ SD.

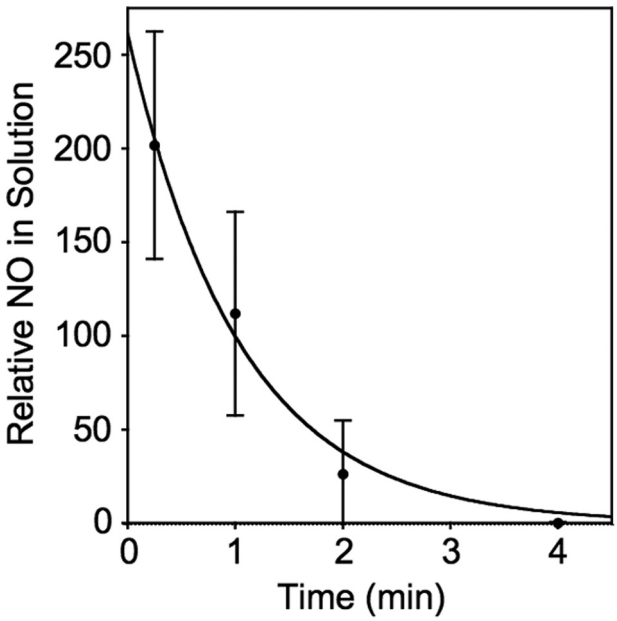

Fig. S4. Quantification of NO in solution. Time course of NO in solution after addition of 1 μM PROLI/NO to buffer at 37 °C. By 4 min NO has decayed such that it is no longer detectable by the NOA. Data are presented as means ± SD.